OPTICAL MODULATION IN RING RESONATORS WITH A SINGLE-DRIVE PUSH-PULL MZI COUPLER

Linjie Zhou, Rui Yang, Haike Zhu, Yanyang Zhou, and Jianping Chen*

State key Laboratory of Advanced Optical Communication Systems and Networks
Department of Electronic Engineering, Shanghai Jiao Tong University, Shanghai 200240, P. R. China
*ljzhou@sjtu.edu.cn

ABSTRACT

We demonstrate low-voltage modulation in a silicon microring resonator integrated with a single-drive push-pull Mach-Zehnder coupler. 20 Gb/s on-off keying (OOK) and 28 Gb/s binary phase-shift keying (BPSK) modulations are achieved with 0.4 V and 3 V drive voltages, respectively.

Keywords: *Optical modulators, Ring resonators, Integrated optical devices.*

1. INTRODUCTION

A high-speed low-power optical modulator is one of the crucial building blocks for transmitters in telecom and datacom applications. Bulk silicon does not possess linear electro-optic effect, and therefore high speed modulation in silicon is routinely realized by using free carrier plasma dispersion effect. There are two types of commonly used modulator structures based on Mach-Zehnder interferometers (MZI) [1-3] and ring/disk resonators [4-6]. Ring modulators have the merits of compact size, low drive voltage, and low power consumption. To implement ring modulators, intracavity refractive index, loss or coupling between ring and bus waveguide can be modulated. Coupling modulation can break the cavity lifetime limitation to enable high speed modulation in high-Q resonators [7-10]. As the output power on resonance is quite sensitive to coupling, slight variation in coupling can result in dramatic output power change near critical coupling [11], facilitating on-off keying (OOK) modulation. It is also beneficial to reduce drive voltage and power consumption while maintain high speed using coupling modulation. A π radian phase flip occurs when the resonance crosses the critical coupling point. This feature can be utilized to generate binary phase-shift keying (BPSK) modulation. As phase changes abruptly, the output modulated signal is chirp free and more tolerant to drive signal imperfections.

In this work, we present a ring modulator with coupling modulation enabled by a single-drive push-pull travelling electrode. Experiments show that 20 and 32 Gbps OOK modulations are realized with 0.4 and 1 V peak-to-peak drive voltages, respectively, and 28 Gb/s BPSK modulation is realized with a 3 V drive voltage.

2. DEVICE STUCTURE

Figure 1(a) shows the schematic structure of the modulator. Input laser light goes through the first 3-dB multimode interference (MMI) coupler and is split into two branches. The light is then modulated by the RF signal applied onto the single-drive push-pull traveling wave electrode (TWE) with its cross-section shown by Fig. 1(b). The modulated light combines at the second 3-dB coupler with one output fed back to the input coupler, forming a circular loop. It can be regarded as a ring resonator coupled to a bus waveguide via a MZI coupler. The coupling is modulated by the TWE, leading to intensity or phase modulation at the output port. When the coupling strength is balanced by the ring inner loss, a critical coupling condition is reached, where the output power is zero. Slight variation of coupling will bring the ring into an over-coupling or under-coupling regime with raised transmission power. It should be noted the phase is changed by π radian when the resonance is switched between over-coupling and under-coupling.

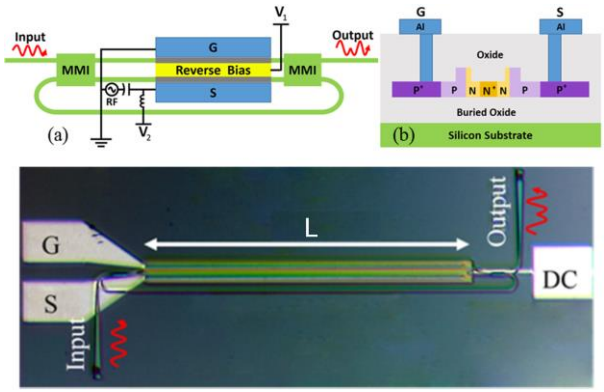

Fig. 1 (a) Schematic of the ring modulator. (b) Cross-sectional view of the MZI modulation arms. (c) Optical microscope image of the fabricated device.

The dimension of silicon waveguides is 220 nm (height) × 500 nm (height) with a 60 nm thick slab. The top arm of the MZI coupler is 5.5 μm longer than the

978-1-4673-7373-9/15/$31.00 ©2015 IEEE

bottom one. The ring radius is 20 μm. The active arms are embed with lateral P-N junctions. The doping concentrations are ~4×10^{17} cm^{-3} and ~1×10^{18} cm^{-3} for the N and P regions, respectively. In the slab beside the P-N junctions are heavily doped N^+ and P^+ regions with a concentration of ~1×10^{20} cm^{-3} for good ohmic contact.

The P^+ regions are connected to the signal (S) and ground (G) metal lines of the TWE, and the N^+ region is connected a DC bias line. During operation, the DC line is applied a positive voltage V_1 to reverse bias the P-N junctions. An RF signal combined with another DC voltage V_2 through a bias-tee is applied to the TWE. The usage of two DC voltage sources is to independently set the reverse biases of the two P-N junctions with top arm biased at $-V_1$ and the bottom arm $-(V_1-V_2)$.

The device was fabricated by the foundry of IME Singapore. Figure 1(c) shows the photograph of the fabricated device. Grating couplers are used for input and output coupling with single mode fibers.

3. STATIC CHARACTERIZATION

Figure 2 shows the measured transmission spectrum normalized to a straight test waveguide with V_1 =1.5 V and V_2 = 0 V. Periodic resonance notches are observed with a free spectral range (FSR) of 0.28 nm. The resonance extinction ratio (ER) decreases from ~35 dB at short wavelengths to ~10 dB at long wavelengths. It is caused by the wavelength dependent coupling of the asymmetric MZI coupler. The inset depicts the evolution of spectrum around the 1544.3 nm resonance with V_2 changing from 0 V to -5 V. It can be seen that the resonance ER reaches the maximum at -4 V where critical coupling is nearly satisfied. Therefore, by manipulating the two DC voltages, we can tune each resonance into critical coupling.

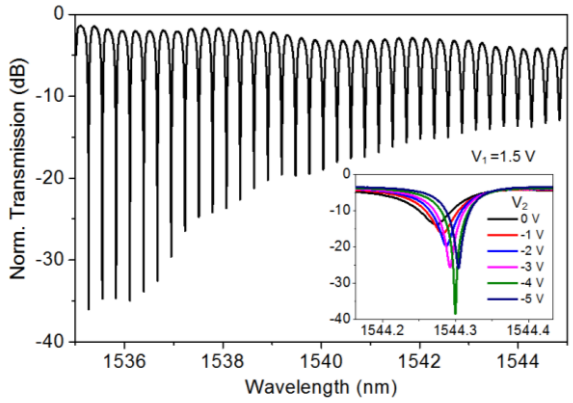

Fig. 2 Measured transmission spectrum with V_1 = 1.5 V and V_2 = 0 V. Inset: resonance tuning around 1544.3 nm with V_2 changing from 0 V to -5 V.

4. MODULATION CHARACTERIZATION

We then characterized the high speed performance of the modulator. A pseudo-random binary sequence (PRBS) signal with a length of 2^{31}-1 generated by a pulse pattern generator (PPG) was used as the RF signal. The RF signal was applied onto the TWE via a 40 GHz GS microwave probe. The modulated optical signal was amplified by an erbium-doped optical fiber amplifier (EDFA) to compensate for the modulator insertion loss and followed by a 1-nm bandwidth optical filter. The amplified optical signal was either connected to a 50 GHz optical oscilloscope for eye diagram measurement or to an optical modulation analyzer (OMA) for decoding and constellation diagram measurement.

4.1 OOK modulation

Figure 3 shows the measured OOK eye diagrams for the modulator with active arm length L = 800 μm. The DC bias voltage is V_1 = 4 V and V_2 = 0 V. A very small RF peak-to-peak voltage of V_{pp} = 0.4 V is enough to drive the modulator. Clean open eye diagrams are observed at data rates of 10 and 20 Gbps with modulation ER of 1.9 and 1.7 dB, respectively. Because of the coupling modulation, output transmission is quite sensitive to phase difference between the active arms, which therefore dramatically reduces the drive voltage and power consumption. To improve the modulation ER, we used a higher drive voltage of V_{pp} = 1 V. The modulation ER is increased to 4.6 dB at 20 Gbps. We got open eye diagram at an ever high date rate of 32 Gbps with ER of 4.2 dB. We also measured the eye diagrams for a modulator with a shorter arm length of 200 μm. Figure 4 shows the eye diagrams at 20 and 32 Gbps with ER of 1.6 and 1.5 dB, respectively.

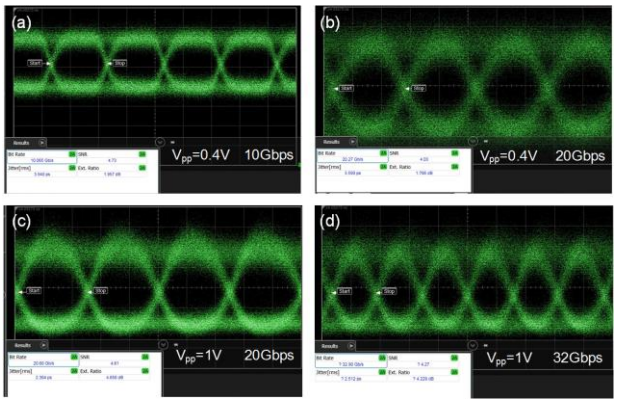

Fig. 3 Measured OOK eye diagrams for a modulator with active arm length 800 μm.

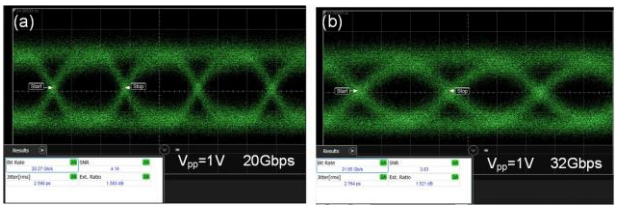

Fig. 4 Measured OOK eye diagrams for a modulator with active arm length 200 μm.

978-1-4673-7373-9/15/$31.00 ©2015 IEEE

4.2 BPSK modulation

Different from OOK modulation, BPSK modulation needs stricter bias setting to operate on critical coupling. In our experiment, we set $V_1 = 1.5$ V and $V_2 = -4$ V. The RF drive signal is $V_{pp} = 3$ V and the received optical power is 1.85 dBm. Figure 5(a) show the BPSK eye diagram measured by the oscilloscope. Figures 5(b) and 5(c) show the decoded constellation diagram and eye diagram measured by the OMA, respectively. The eye diagram exhibits a Q-factor of 6.3 dB and an error vector magnitude (EVM) of 23.3%. The bit error rate (BER) estimated from the EVM is around 8e-10.

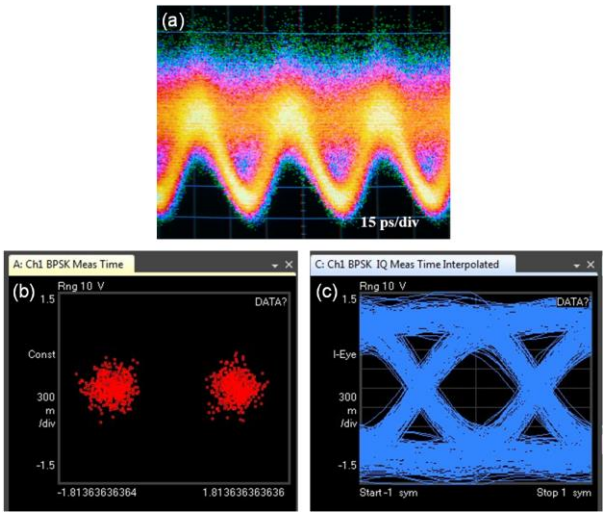

Fig. 5 Measured BPSK signals: (a) eye diagrams, (b) constellation diagram, and (c) decoded eye diagram.

5. CONCLUSION

We have demonstrated OOK and BPSK modulation using ring modulators integrated with a single-drive push-pull coupler. Coupling modulation provides several advantages over intra-cavity index and loss modulations, including low chirp, low drive voltage, large tolerance to drive signal fluctuation for BPSK, and high speed beyond cavity lifetime limitation. With a single drive TWE electrode and two DC biases, we can freely set each resonance condition to switch between OOK and BPSK modulation formats. Our measurements show that OOK modulation can be realized with a RF drive signal as low as 0.4 V at 20 Gbps and BPSK modulation realized at 28 Gbps with a drive signal of 3 V.

6. ACKNOWLEDGMENTS

This work was supported in part by the 973 program (ID2011CB301700), the 863 program (2013AA014402), the National Natural Science Foundation of China (NSFC) (61422508) and SRFDP of MOE (Grant No. 20130073130005). We also acknowledge IME Singapore for device fabrication.

7. REFERENCES

[1] J. Wang, L. Zhou, H. Zhu, R. Yang, Y. Zhou, L. Liu, *et al.*, "Silicon high-speed binary phase-shift keying modulator with a single-drive push-pull high-speed traveling wave electrode," *Photon. Res.,* vol. 3, pp. 58-62, 2015.

[2] H. Zhu, L. Zhou, T. Wang, L. Liu, Y. zhou, J. Wang, *et al.*, "50 Gb/s silicon QPSK modulator with single-drive push-pull traveling wave electrodes design," in *Asia Communications and Photonics Conference*, Shanghai, 2014, p. AF1A.2.

[3] P. Dong, L. Chen, and Y.-k. Chen, "High-speed low-voltage single-drive push-pull silicon Mach-Zehnder modulators," *Opt. Express,* vol. 20, pp. 6163-6169, 2012.

[4] L. Zhou and A. W. Poon, "Silicon electro-optic modulators using pin diodes embedded 10-micron-diameter microdisk resonators," *Opt. Express,* vol. 14, pp. 6851-6857, 2006.

[5] X. Xiao, H. Xu, X. Li, Y. Hu, K. Xiong, Z. Li, *et al.*, "25 Gbit/s silicon microring modulator based on misalignment-tolerant interleaved PN junctions," *Opt. Express,* vol. 20, pp. 2507-2515, 2012.

[6] Q. Xu, S. Manipatruni, B. Schmidt, J. Shakya, and M. Lipson, "12.5 Gbit/s carrier-injection-based silicon micro-ring silicon modulators," *Opt. Express,* vol. 15, pp. 430-436, 2007.

[7] W. D. Sacher, W. M. Green, D. M. Gill, S. Assefa, T. Barwicz, M. Khater, *et al.*, "Binary phase-shift keying by coupling modulation of microrings," *Opt. Express,* vol. 22, pp. 20252-20259, 2014.

[8] W. Sacher, W. Green, S. Assefa, T. Barwicz, H. Pan, S. Shank, *et al.*, "Coupling modulation of microrings at rates beyond the linewidth limit," *Opt. Express,* vol. 21, pp. 9722-9733, 2013.

[9] L. Sun, T. Ye, X. Wang, L. Zhou, and J. Chen, "Chirp-free optical return-to-zero modulation based on a single microring resonator," *Opt. Express,* vol. 20, pp. 7663-7671, 2012.

[10] T. Wang, M. Xu, F. Li, J. Wu, L. Zhou, and Y. Su, "Design of a high-modulation-depth, low-energy silicon modulator based on coupling tuning in a resonance-split microring," *J. Opt. Soc. Am. B,* vol. 29, pp. 3047-3056, 2012.

[11] L. Zhou and A. W. Poon, "Electrically reconfigurable silicon microring resonator-based filter with waveguide-coupled feedback," *Opt. Express,* vol. 15, pp. 9194-9204, 2007.

978-1-4673-7373-9/15/$31.00 ©2015 IEEE